In utero sFlt-1 exposure differentially affects gene expression patterns in fetal liver

V. Stojanovska[1], K. M. Holwerda[2], A. M. van der Graaf[3], R. N. Verkaik-Schakel[1],
M. V. Boekschoten[4], M. M. Faas[3], S. A. Scherjon[1] and T. Plösch[1]

[1]Department of Obstetrics and Gynecology, University of Groningen, University Medical Center Groningen, The Netherlands, [2]Department of Pathology and Medical Biology, University of Groningen, University Medical Center Groningen, The Netherlands, [3]Department of Pathology and Medical Biology, Division of Medical Biology, University of Groningen, University Medical Center Groningen, The Netherlands and [4]Nutrition, Metabolism and Genomics Group, Division of Human Nutrition, Wageningen University, The Netherlands

Original Article

Abstract

The soluble fms-like tyrosine kinase factor 1 (sFlt-1) is a major contributor to antiangiogenesis during preeclampsia. However, little is known about the effects of sFlt-1 on fetal health. In this study we aim to evaluate the effects of the sFlt-1 concentration during pregnancy on fetal liver physiology. We used adenoviral gene delivery in Sprague-Dawley dams (seven females, 10 weeks old) during mid-gestation (gestational day 8) with adenovirus overexpressing sFlt-1, and age-matched controls (six females, 10 weeks old) with empty adenoviral virus in order to quantify the sFlt-1 concentrations in pregnant dams. Dams exposed to adenoviral sFlt-1 delivery were subdivided into a low ($n = 4$) and high sFlt-1 ($n = 3$) group based on host response to the virus. One-way analysis of variance showed that fetuses (five per dam) exposed to high sFlt-1 concentrations *in utero* show fetal growth restriction (1.84 ± 0.043 g high sFlt-1 *v.* 2.32 ± 0.036 g control; mean (M) $\pm$ S.E.M.; $P < 0.001$), without hypertension or proteinuria in the dams. In continuation, the microarray analysis of the fetal liver of the high sFlt-1 group showed significant enrichment of key genes for fatty acid metabolism and Ppara targets. In addition, using pyrosequencing, we found that the Ppara enrichment in the high sFlt-1 group is accompanied by decreased methylation of its promoter (1.89 ± 0.097 mean % methylation in high sFlt-1 *v.* 2.26 ± 0.095 mean % methylation in control, M $\pm$ S.E.M., $P < 0.02$). Our data show that high sFlt-1 concentrations during pregnancy have detrimental effects on the fatty acid metabolism genes and the Ppara targets in the fetal liver.

Introduction

The fetal programming hypothesis proposes that an adverse intrauterine and early-life environment can shape the individual toward susceptibility to cardiometabolic diseases.[1] This concept is supported by many studies that have shown that malnutrition, toxins, smoking and maternal diseases during pregnancy affect the birth weight of the offspring, resulting in an aberrant response of the cardiovascular and metabolic system in later life.[2–5] Furthermore, the opposite situation of increased birth weight or macrosomia also contributes to metabolic programming and later-life morbidity, primarily via altered body composition at birth.[6–8]

Preeclampsia is a pregnancy-associated disorder, usually complicated with fetal growth restriction and affects 3–7%[9] of the population worldwide. It is diagnosed with hypertension and proteinuria and poses a major threat to the maternal and fetal health.[10] As a multifactorial disease, it is associated with several pathophysiological pathways including angiogenic imbalance with a predominance of soluble fms-like tyrosine kinase-1 (sFlt-1), which increased two- to five-fold in preeclamptic patients.[9,11] sFlt-1 serves as an antagonist to placental growth factor (PlGF) and vascular endothelial growth factor (VEGF), thus promoting hypovascularization, endothelial dysfunction and vasoconstriction in the mother with concomitant hypoxia.[12]

Recent studies suggest that sFlt-1 may play a role in lipid and protein metabolism. The circulating plasma proteome of the dams exposed to sFlt-1 shows increased apolipoprotein fractions that are mediators of cholesterol esterification and removal of excess cholesterol from tissues.[13] Moreover, the fatty acid availability is increased in sFlt-1-induced preeclampsia due to increased expression of fatty acid translocase in sFlt-1 overexpressing placental tissue.[14] Additionally, it was reported that the liver X receptor and retinoid X receptor (LXR/RXR) pathway is upregulated in sFlt-1-induced preeclampsia which is a substantial pathway in the regulation of lipid metabolism and inflammation.[13]

Although increased concentrations of sFlt-1 contribute to the pathogenesis of preeclampsia and fetal growth restriction,[15] the specific effects of sFlt-1 on the developing fetus are not well

CAMBRIDGE
UNIVERSITY PRESS

understood. With this study, we aimed to evaluate the following: (1) the effects of sFlt-1 on the fetal development, (2) effects on fetal liver gene expression and (3) whether prominent changes in gene expression are accompanied by changes in DNA methylation.

Materials and methods

Animals

All animals were housed and handled according to institutional guidelines following Dutch legislation. All experiments were approved by the Animal Ethics Committee of the University of Groningen. Female Sprague-Dawley (SD) rats of 10-weeks-old (Charles River, France) were housed in a light and temperature-controlled facility (lights on from 7:00 am to 7:00 pm, 21°C). Food and water were provided *ad libitum*. Vaginal smears were taken daily. When the females were in a pro-estrus phase of their cycle, they were housed with a male overnight. The following day, if spermatozoa were present in the vaginal smear, then it was considered day 0 of gestation. At day 8 of gestation, animals were randomly divided into two groups: control ($n = 6$) and sFlt-1 ($n = 7$), receiving either control Ad-null or adenovirus over-expressing sFlt-1 (Ad-sFlt-1), respectively. We distinguished either ultra-high (>1000 ng/ml) or very low (<1000 ng/ml) sFlt-1 plasma concentrations in our sFlt-1 group, and we continued the analysis with high ($n = 3$) and low sFlt-1 ($n = 4$) group of dams.

Amplification and purification of sFlt-1 and control adenovirus

Adenovirus vector stock of Ad-null (a kind of gift from U.J. Tietge, University Medical Center Groningen, the Netherlands) and Ad-sFlt-1 (a kind of gift from S.A. Karumanchi, Beth Israel Deaconess Medical Center, Boston, MA, USA) were used for adenoviral gene delivery. Viruses were amplified in HEK 293A cells at a multiplicity of infection of 10. Adenoviral purification was performed with a cesium chloride (CsCl) density gradient ($d = 1.45$ and $1.20\,g/ml$). The clear thick adenoviral band was transferred to a DG column (Biorad, Temse, Belgium) for washing and elution. The titer of plaque-forming units (PFU) was analyzed with an enzyme-linked immunoassay that detects the adenoviral hexon (Adeasy viral titer kit, Agilent Technologies, Santa Clara, CA, USA), and 1×10^{12} PFU of adenovirus expressing mouse sFlt-1 or the empty vector were injected via the tail vein on gestational day (GD) 8.

Blood pressure measurements

On GD19, the systemic blood pressure for all groups was assessed under anesthesia (100% O_2, 0.8 ml/min, 5% isoflurane for induction followed by 2%) with the aortal catheter positioned in the abdominal aorta and connected with a bed-side monitor (Datex-Ohmeda, Cardiocap/5). Blood pressure measurement values were recorded 30 s after cannulation.

Analysis of blood and urine samples

On GD12, maternal blood was collected in ethylenediaminete-traacetic acid containing tubes via the tail vein. Within half an hour the blood was centrifuged for 20 min at 1000 rpm and the plasma was stored at −80°C until analysis. On GD19, animals were anesthetized with isoflurane inhalation and the abdominal cavity was opened. After blood pressure measurements, blood was collected via the abdominal aorta and centrifuged as stated above to collect plasma. Plasma was stored as stated earlier. Fetal blood was collected by nicking the left ventricle of the heart, while the fetuses were slightly tilted in order to keep the pooled blood in the thoracic cavity, and it was collected in heparin-coated capillary tubes (Vitrex Medical A/S, Herlev, Denmark). sFlt-1 concentrations in plasma were determined using a mouse sFlt-1 enzyme-linked immunosorbent assay kit (R&D Systems, Inc., Minneapolis, MN, USA). A total of 24 urine samples were collected by placing the pregnant dams in metabolic cages at GD16 and 17, and the protein levels were determined using Pierce method. The concentration of proteins (mg) per sample was multiplied by the 24-h urine volume.

RNA isolation

Total RNA was isolated from fetal livers collected on GD19 with allprep DNA/RNA mini kit (Qiagen, Venlo, the Netherlands), following the manufacturer's protocol. RNA quality and quantity were assessed with Nanodrop 2000c (Thermo Scientific, Pittsburgh, PA, USA). RNA was immediately stored at −80°C until further analysis. RNA integrity was further verified on an Agilent 2100 bioanalyzer, using the Eukaryote total RNA nano assay according to manufacturer's protocol (Agilent Technologies, Amsterdam, the Netherlands). Samples that had an RNA integrity number >9.0 and no RNA degradation products were considered acceptable for microarray hybridization.

Microarray hybridization and analysis

Total RNA isolated from fetal livers (five samples per group: control and high sFlt-1) was used for microarray analysis. Labeled cDNA was prepared from 100 ng RNA using the Ambion Whole Transcript Expression Kit (Life Technologies, Carlsbad, CA, USA) and Affymetrix GeneChip WT Terminal Labeling Kit (Affymetrix, Santa Clara, CA, USA). All samples were hybridized to Affymetrix GeneChip Mouse Gene 1.1 ST arrays according to standard Affymetrix protocols. Array images and normalization was performed with Bioconductor software packages (Lin 2011). Probes sets were assigned to unique gene identifiers (IDs) of the Entrez Gene database, resulting in 19.357 assigned Entrez IDs.

Bioinformatics analysis

The microarray covered 19.357 genes, and only the ones with an intensity value of >20 on at least three arrays and interquartile range (IQR) >0.2 on at least five probes per gene on the array were selected for further analysis. The top 1000 most variable genes were used for principal component analysis (PCA) using MultiExperiment Viewer version 4.8.4. Signal log2 ratios, which represent fold changes, and related significances of change were calculated from the mean intensities of the control and high sFlt-1 group using intensity-based moderated t statistics implementing Bayes correction.[16] Resulting log2 ratios and *P*-values were applied for further analysis of the data. Gene set enrichment analysis (GSEA) was used to relate the microarray data to networks of diseases and biological functions. Heat maps generation showing a comparison of gene expression patterns was done with MultiExperiment Viewer version 4.8.4.

Real-time quantitative polymerase chain reaction analysis

Of total RNA, 1 µg was used for cDNA conversion with reagents from Invitrogen (Invitrogen, USA), according to manufacturer's recommendations. Real-time quantitative polymerase chain reaction (qPCR) was performed using PowerUp SYBR green master mix (Applied Biosystems, Foster City, CA, USA) on StepOnePlus real-time PCR system (Applied Biosystems) with the following settings: 20 s 95°C, 40 cycles at 95°C for 1 s and at 60°C for 20 s. Multiexon spanning PCR primers (sequences available at rtprimerdb.org) were designed with Primer Express Software (Applied Biosystems) and synthesized by Eurogentec (Seraing, Belgium). The average expression level of *36b4* and *Gapdh* was used as a housekeeping gene in all qPCR analysis and the ddCt method was used for quantification.

Genomic DNA isolation and pyrosequencing

Fetal livers were homogenized with a TissueLyser LT (Qiagen) for 1 min at 40 Hz. Genomic DNA was isolated using allprep DNA/RNA mini kit (Qiagen), following manufacturer's protocol. DNA purity and concentration were validated on Nanodrop 2000c, while 500 ng of genomic DNA was used for bisulfite conversion with the EZ DNA methylation gold kit (Zymo Research, Leiden, the Netherlands) according to manufacturer's protocol. Samples were stored at −20°C until analysis. With Pyromark Assay Design 2.0 software (Qiagen), bisulfite specific primers were designed for the rat *Ppar* alpha promoter region (forward: 5′-biotin-GAGGG-TATTAGGTGGGA AGTTTTATTAG-3′; reverse: 5′-AACC-TAAAAAACCCTAAACA ATTCT-3′). Bisulfite-modified DNA of 20 ng were used for amplification with HotStarTaq master mix using the following steps: DNA polymerase activation (95°C for 15 min), three-step cycle of denaturation (94°C for 30 s), annealing (58°C for 1 min) and extension (72°C for 45 s) repeated for 45 cycles in a row. Finally, the last extension was carried out at 72°C for 7 min. The PCR product was analyzed using the sequencing primer: 5′-CTAAATAAAAAAACTACCCAAAAT-3′ and sequence-to-analyze: CACCCRACRA ACRAAACAAC CCTA-TAAAAA AAAC RCRCCT AAACRAACRC RCCTTTCTAC TCCCAACCCC RCRCACCR, for the extent of methylation per selected CpG position by pyrosequencing using a Pyromark Q24 system and analysis software 2.0 (Qiagen). The level of DNA methylation is given as a percentage.

Statistical analysis

All data are presented as M ± S.E.M. Differences between groups were calculated with an unpaired *t*-test (two groups) or one-way analysis of variance (ANOVA) (three groups). Comparison of multiple groups (DNA methylation analysis of different CpG positions) was analyzed by two-way ANOVA, followed by a Bonferroni *post-hoc* test. For all statistical tests, a *P*-value <0.05 was considered significant. All data were analyzed using GraphPad Prism 6.0 Software (GraphPad).

Results

Maternal characteristics upon sFlt-1 overexpression

To validate our overexpression model, we measured sFlt-1 concentrations in plasma, 96 h post adenovirus injections (GD12) and at GD19. Surprisingly, plasma sFlt-1 concentrations in the overexpressed animals were not in the same range. As

presented in Fig. 1a, some dams showed a moderate increase (*n* = 4) of sFlt-1 concentrations in plasma (sFlt-1 at GD12: 310 ± 109 ng/ml and at GD19: 640 ± 624 ng/ml), whereas other dams (*n* = 3) showed high sFlt-1 concentrations (at GD12: 1073 ± 735 ng/ml; and at GD19: 4726 ± 2215 ng/ml). In that way, we characterized two groups of dams with low and high sFlt-1 concentrations in addition to the control group, where the sFlt-1 concentrations at GD19 were almost zero (0.08 ± 0.008 ng/ml). No statistical analysis was performed for the data presented in Fig. 1a, as the primary purpose was to show increase of sFlt-1 concentrations after sFlt-1 adenoviral overexpression. In addition, at GD19 the aortic blood pressure was assessed, and there were no significant differences between the control and low sFlt-1 group. In comparison, the high sFlt-1 group showed decreased diastolic and mean arterial pressure (Fig. 1b). Furthermore, excessive proteinuria was not present in any of the inspected groups (Fig. 1c).

Fetuses from dams that have high sFlt-1 concentrations are growth restricted

It has been reported that increased sFlt-1 concentrations in the mother can result in growth restriction of the fetus.[15] In our
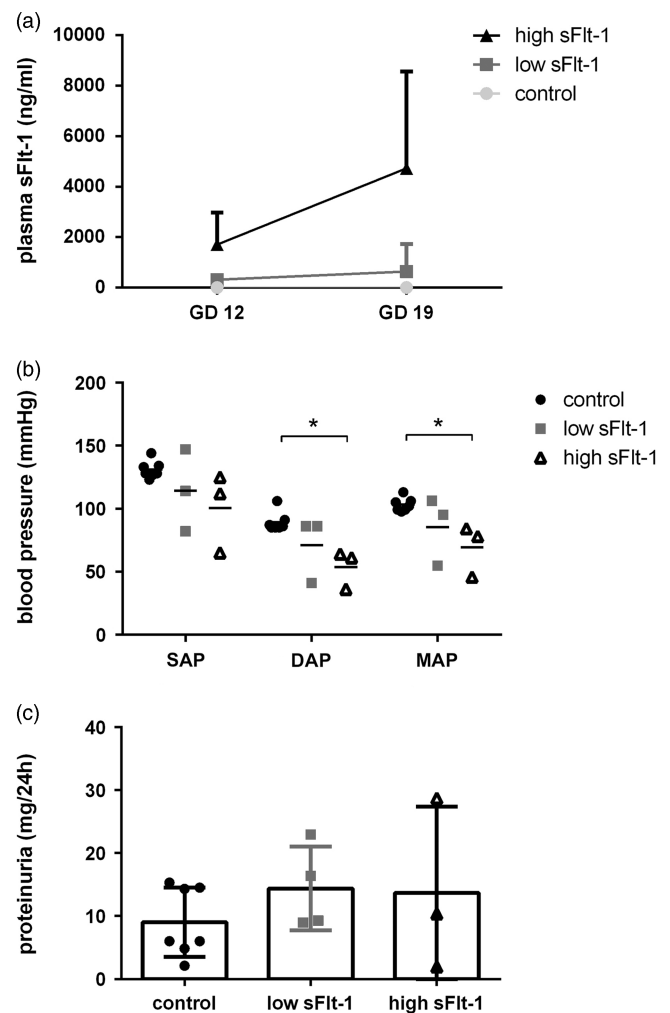

Fig. 1. Overexpression of sFlt-1 in pregnant dams. (a) Plasma sFlt-1 concentrations in dams (*n* = 3,4), (b) blood pressure values (*P < 0.05, *n* = 3,4), (c) protein levels in 24 h urine from pregnant dams (*n* = 3,4).

study, fetuses that were exposed to high sFlt-1 concentrations were approximately 22% lighter and the length was reduced by 9% in comparison to controls. Also, the body proportionality, as expressed by the ponderal index (weight in grams/length in mm), was lower in the fetuses exposed to high sFlt-1 concentrations when compared to the fetuses exposed to low or no sFlt-1 (Fig. 2a–c). There were no differences between these parameters in the control and the low sFlt-1 group (Fig. 2).

Brain-sparing and increased sFlt-1 concentrations in fetuses exposed to high sFlt-1 maternal concentrations

To evaluate whether the fetal growth restriction is asymmetrical or symmetrical, we assessed the organ weight at GD19. The liver weights of fetuses exposed to high maternal sFlt-1 concentrations were smaller in comparison to the control group (Fig. 3a). Brain weight was uncompromised in all groups (Fig. 3b). We also checked the brain/liver ratio as an indicator of fetal asymmetrical/symmetrical growth. We observed increased brain/liver ratio in the fetuses exposed to high sFlt-1 as compared with the low sFlt-1 and the control group and no changes in the low sFlt-1 group as compared with the control group (Fig. 3c), indicating that brain-sparing occurs in the fetuses exposed to the high sFlt-1. To
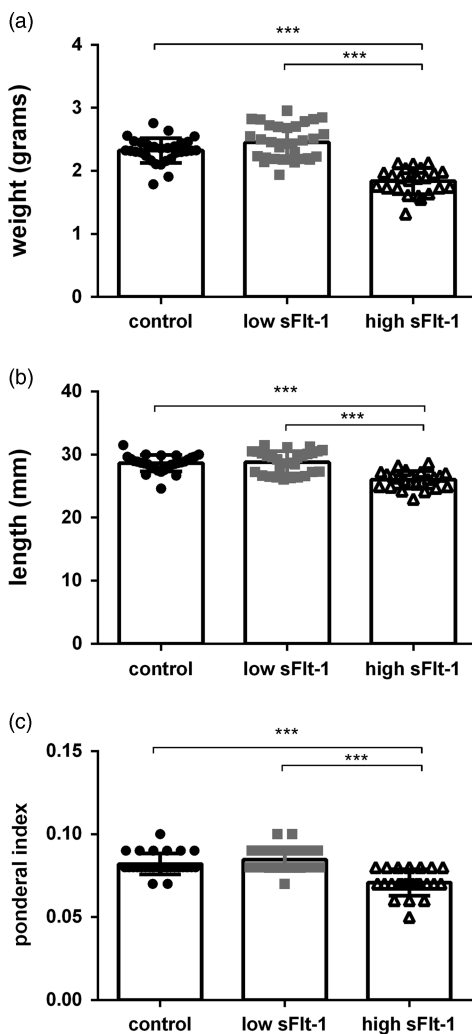
evaluate whether the maternal sFlt-1 levels could interfere the fetal sFlt-1 levels, we measured the plasma sFlt-1 levels in the fetuses to confirm the difference in the sFlt-1 exposure of the fetuses. We observed that fetuses exposed to high sFlt-1 during pregnancy have an 18-fold increase of sFlt-1 in fetal plasma in comparison to control and low sFlt-1 group (Fig. 3d).

sFlt-1 overexpression and growth restriction modulate the fetal liver gene expression

In order to detect whether the fetal growth restriction due to the sFlt-1 overexpression affected the liver function, we performed microarray analysis on fetal liver RNA. We performed an unsupervised clustering analysis of the top 1000 most variable genes based on IQR, which is an indicator of variability of gene expression. In continuation, we performed PCA of the top 1000 most variable genes. As shown in Fig. 4a, the samples tend to cluster in two separate clusters in principle component 1 (PC1), which accounts for 34% of the gene expression. Only one fetal liver from the high sFlt-1 group tends to cluster with the control ones. The dendrogram plot, accompanied by a heat map of the gene expression differences between the groups, is presented in Fig. 4b. As expected, the liver gene expression profiles between the groups were recognizably different; that is exposure to high sFlt-1 concentrations *in utero* can mediate fetal liver molecular changes. Further analysis depicted that there is upregulation of several genes involved in fatty acid β-oxidation, including the master regulators such as *Cpt1a*, *Cpt1b* and *Acadvl*. Furthermore, we have validated the microarray data with qPCR analysis of eight target genes of the Ppara transcription factor in fetal livers (Fig. 5). As expected, seven out of eight genes showed increased levels only in the group of fetuses exposed to the high sFlt-1 concentrations in the mother.

Fatty acid metabolic pathways are upregulated in liver from growth-restricted fetuses exposed to high sFlt-1 concentrations

Since many genes were upregulated in the high sFlt-1 fetal livers as compared to the control fetal livers (Fig. 4b and 4c), we performed a GSEA in order to evaluate the pathways in which these genes are involved. We used GSEA to analyze GO and KEGG gene sets that are significantly altered in the livers from the high sFlt-1 group in comparison to the controls. Top downregulated pathways involved olfactory sensing pathways and g-gated potassium and calcium channels (Supplementary Table 1). Moreover, significantly enriched metabolic pathways included genes responsible for fatty acid β-oxidation, fatty acid, triacylglycerol and keto body metabolism (Table 1). Moreover, GSEA indicated that genes involved in the *Ppara* signaling pathway are induced upon sFlt-1 overexpression (Table 1).

Ppara is differentially methylated in fetal liver upon fetal growth restriction due to sFlt-1 overexpression

Moreover, it has been reported that protein-restricted diet during pregnancy influences the methylation rates of the *Ppara* promoter region in livers from juvenile offspring.[17] To investigate whether the methylation status of *Ppara* is influenced in our growth-restricted and sFlt-1-exposed fetuses, we designed a rat-specific pyrosequencing assay for *Ppara* that encompasses 10 CpG positions located 500 bp upstream the transcriptional start site (Fig. 6a). Methylation of CpG position 5 was decreased in the high sFlt-1
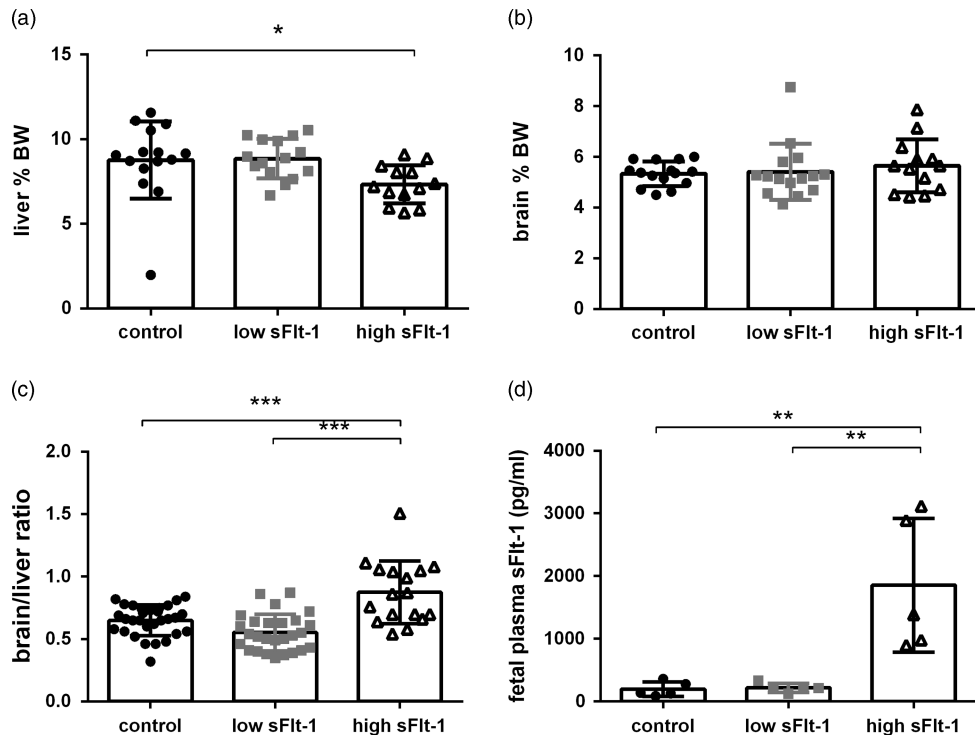

Fig. 2. Fetal characterization. (a) Fetal body weight at GD19 ($n = 10$), (b) fetal crown-rump length at GD19 ($n = 10$), (c) fetal weight to length ponderal index ($n = 10$). ***$P < 0.001$.

Fig. 3. Asymmetrical growth restriction in fetuses exposed to high sFlt-1. (a) Fetal liver weight as percentage of body weight at GD19 ($n = 10$), (b) fetal brain weight as percentage of body weight at GD19 ($n = 10$), (c) brain to liver ratio ($n = 10$), (d) fetal plasma sFlt-1 concentrations at GD19 ($n = 10$). *$P < 0.05$, **$P < 0.01$, ***$P < 0.001$.

group (Fig. 6b) and the average methylation of the selected region showed hypomethylation (Fig. 6c), which is in accordance with the previously reported results.

Discussion

The results of the present study indicate that maternal sFlt-1 overexpression has an important implication in the fetal liver physiology. Despite the limited changes in the maternal physiology, exposure to a high sFlt-1 concentration from middle to the end of gestation resulted in fetal growth restriction. This was accompanied with decreased liver weight, altered gene expression and *Ppara* methylation in the fetal liver.

It was reported that sFlt-1 overexpression during pregnancy contributes to the pathophysiology of preeclampsia.[15,18] However, in our study, despite the increased viral load to induce sFlt-1 overexpression, we could not record the clinical symptoms of preeclampsia. One possible explanation could be that our model produced either too high or too low sFlt-1 concentration instead of the middle range concentrations that were obtained with other models.[15,18,19] It can be speculated that these conflicting results are due to the differences in the timing and methods used to track the blood pressure and proteinuria. For example, we avoided usage of telemetry and we primarily assessed the systemic blood pressure via aortal catheter that involves administration of anesthesia to the dams, which might as well contribute to the lower blood pressure values. However, the advantage of this specific model is that we can study the effects of high levels of sFlt-1 on the fetuses in the absence of maternal signs, such as hypertension and proteinuria. Therefore, we consider our models as a model of sFlt-1 overexpression.

Using this maternal sFlt-1 overexpression model, we demonstrate that the increased maternal sFlt-1 concentrations lead to asymmetrical growth restriction of the fetus. This is a condition where the brain development is preserved at the expense of liver growth. The brain-sparing effect usually occurs due to maternal and/or fetal hypoxia where concomitant redistribution of the oxygenated blood is established at the expense of other organs.[20,21] In addition, brain/liver ratio is an important predictor of the fetal outcome.[22] It is well established that redistribution of nutrients leads to a reduction of the functional capacity of metabolically active organs, for example, liver. This adaptation can lead to metabolic programming and a thrifty phenotype that can persist later in life. Several previous studies have shown that low birth weight increases the risk of cardiovascular and metabolic diseases, for example, stroke, diabetes, obesity, etc.[23–27] Potential factors include malnutrition and toxins present during pregnancy. Our data demonstrate that fetal exposure to sFlt-1 is associated with asymmetrical growth restriction, however to what extent this contributes to developmental programming of the fetus still remains to be determined.

sFlt-1 has a molecular weight higher than $5 \, kDa$[28] and in normal physiological conditions does not freely diffuse through the placenta. However, in our study, we observed that maternal plasma sFlt-1 concentrations result in increased plasma sFlt-1 concentrations in the fetuses as well. We speculate that this can be either due to changed permeability of the placenta when the angiogenic balance is disturbed or due to direct exposure of the pup to the sFlt-1 adenoviral delivery. These results support earlier observations that angiogenic factors are increased in maternal and umbilical cord samples in pregnancies complicated with intrauterine growth restriction.[29] Additionally, several other studies have reported that newborns small for gestational age have also increased sFlt-1 concentrations in umbilical plasma samples.[30,31] These results suggest that the fetuses are not only exposed to the indirect effects of sFlt-1 but also via direct exposition to sFlt-1. It
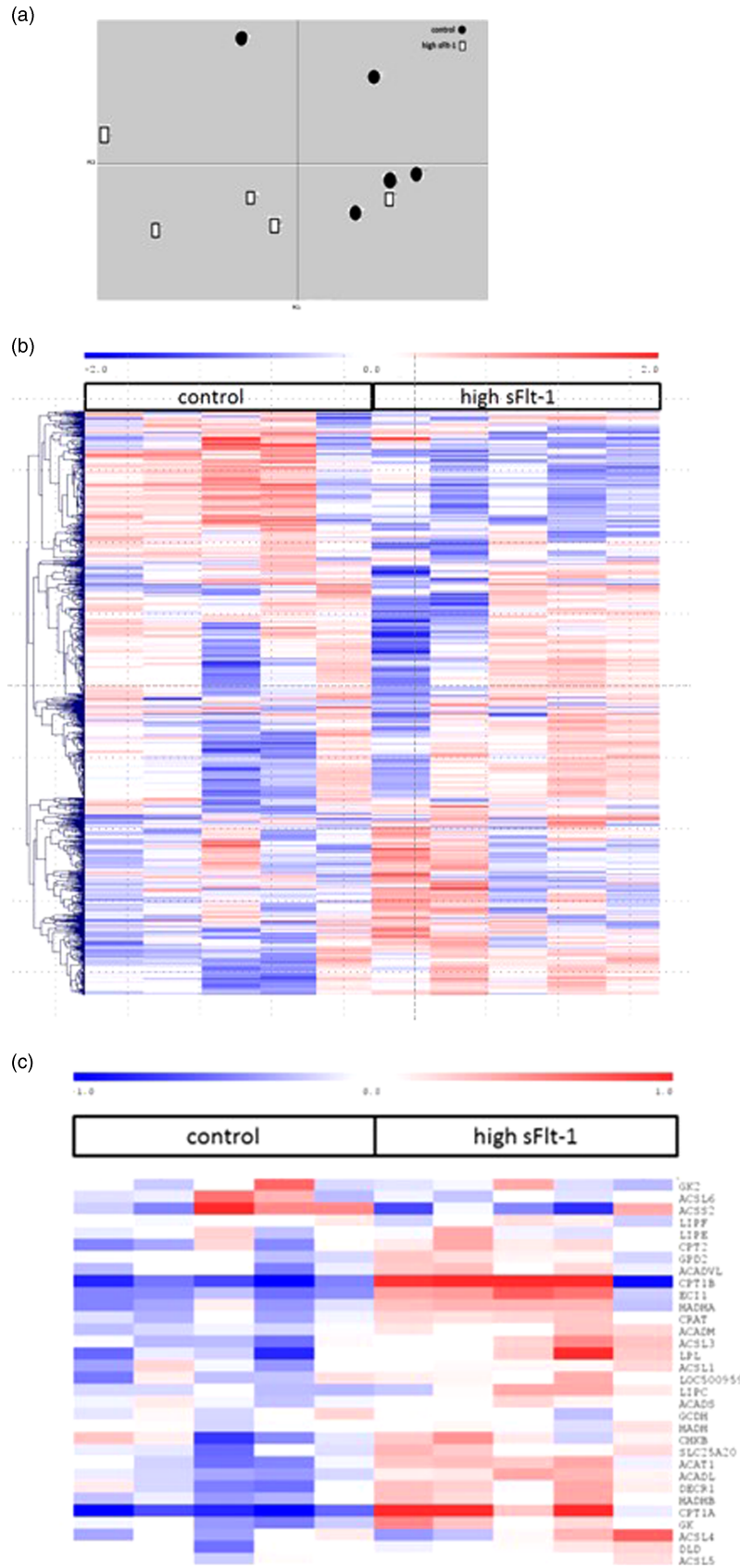
(a)

(b)

(c)

Fig. 4. Analysis of the transcriptional response to high sFlt-1 in fetal liver. (a) Principal component analysis of the top 1000 differentially expressed genes. (b) Heatmap showing top 1000 differentially expressed genes in the liver in response to sFlt-1. (c) Heatmap showing enriched fatty acid β-oxidation gene set.
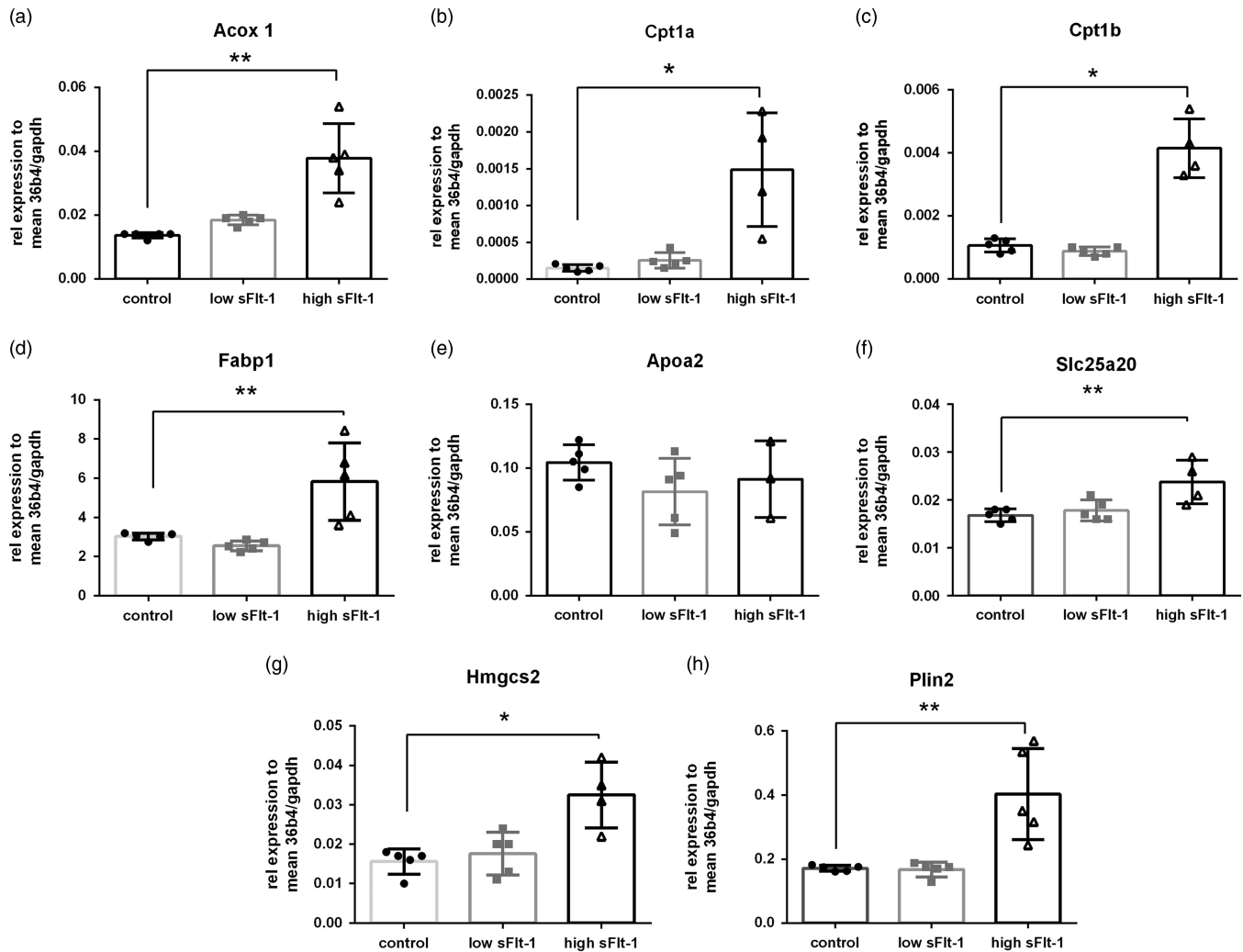
Fig. 5. qPCR validation of eight *Ppara* targets. (a) *Acox1*, (b) *Cpt1a*, (c) *Cpt1b*, (d) *Fabp1*, (e) *Apoa2*, (f) *Slc25a20*, (g) *Hmgcs2* and (h) *Plin2* mRNA levels relative to *36B4* and *Gapdh* in fetal liver. One-way ANOVA, shown M ± S.E.M. *$P < 0.05$, **$P < 0.01$.

Table 1. Gene set enrichment analysis of upregulated pathways in response to high sFlt-1. The normalized enrichment score (NES) and the false discovery rate (FDR) with adjusted *P*-value (or q-value) FDR-q val are indicated in the table. *Ppara* targets are significantly enriched in the fetal liver after exposure to high sFlt-1

Upregulated pathways	Size	NES	FDR q-val
Ppara targets	172	3.329801	<0.00001
Platelet degranulation	70	2.958827	<0.00001
Elastic fiber formation	36	2.888633	<0.00001
KEGG_Fatty acid degradation	45	2.867578	<0.00001
WP1307_Fatty acid β-oxidation	32	2.81599	<0.00001
Extracellular matrix O#	231	2.808842	<0.00001
KEGG_Adherens junction	68	2.747173	<0.00001
Platelet activation signaling and aggregation	200	2.724181	<0.00001
WP506_Fatty acid β-oxidation 1	25	2.708746	<0.00001

is possible that sFlt-1 interferes with the fetal organ angiogenesis, but the exact mechanism will require further investigation.

Importantly, we observed that the gene expression profile is changed in fetal livers that were exposed to high sFlt-1 concentrations *in utero*. The difference was prominent in the genes involved in the fatty acid metabolism, which is crucial for the energy supply of the fast-growing fetal organism. This is in accordance with a mouse study of sFlt-1 overexpression where it was found that the LXR/RXR pathway was the top modified canonical pathway in the plasma proteome of dams 6 months postpartum.[13] The LXR/RXR pathway is involved in the regulation of the lipid metabolism. In contrast, a calorie-restricted diet results in decreased expression of genes involved in fatty acid synthesis[32] and folate-restricted diet increases the expression of genes involved in fatty acid degradation and β-oxidation processes.[33] These findings suggest that expression of modulation of genes involved in fatty acid metabolism serves as a compensatory mechanism in fetal growth restriction, obtained either via nutritional or via antiangiogenic manipulation.

In agreement with the upregulated fatty acid metabolism genes, we observed that the *Ppara* targets pathway was enriched as well. Ppar genes are a unique set of fatty acid-regulated transcriptional factors that increase fatty acid metabolism.[34] In
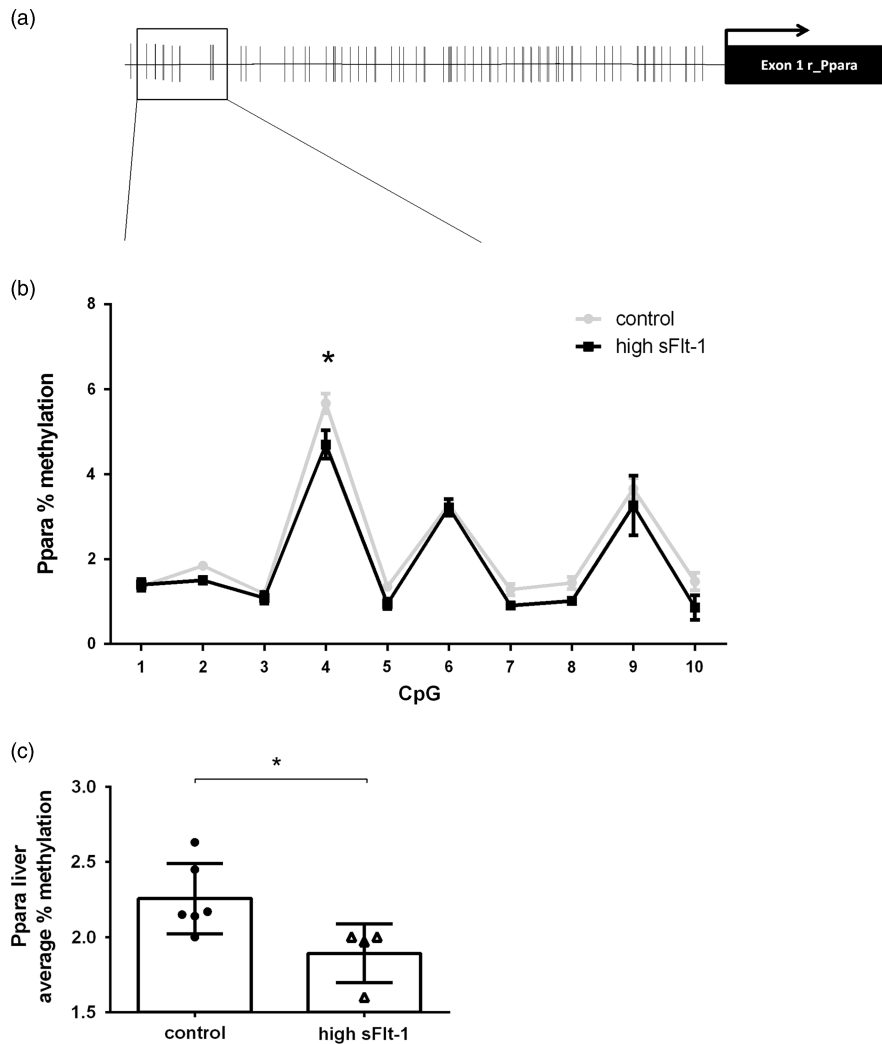
Fig. 6. *Ppara* is differentially methylated in the liver in response to high sFlt-1. (a) Schematic representation of promoter region of rat *Ppara*. (b) Methylation percentage levels per each inspected CpG site ($n = 6$, two-way ANOVA test). (c) Average methylation percentage per inspected area ($n = 6$), $*P < 0.05$.

particular, *Ppara* acts as a key nutritional and environmental sensor in order to establish metabolic adaptation.[35] Activation of *Ppara* induces uptake and catabolism of fatty acids by upregulation of genes involved in β-oxidation and fatty acid transport.[36] Moreover, the peroxisome proliferator-activated receptors have a substantial role in fetal metabolism and are well known for their role in developmental programming.[37]

It has been reported that fetal growth restriction due to a caloric-restricted maternal diet results in decreased *Ppara* expression and can be maintained for longer period of time.[38] However, growth-restricted livers from protein-restricted mothers[17] have increased *Ppara* expression that is in accordance with our results. It appears that the differences in the fatty acid metabolism and *Ppara* signaling are also affected in our sFlt-1-exposed growth-restricted fetuses.

We found moderate but significant changes in the promoter methylation pattern of *Ppara* in the fetal liver exposed to the highest sFlt-1 concentrations *in utero*. Previously, it was reported that *Ppara* is differentially methylated in the offspring livers of growth-restricted rats exposed to low protein and calorie restriction intake *in utero*. In continuation, it was shown that these discrete changes are stable and persistent in adulthood.[17] These *Ppara* methylation differences in early life might be

considered as an indicator of metabolic adaptation to the intrauterine harsh environment.

Together, these results show that high maternal levels of sFlt-1 result in fetal growth restriction, high fetal plasma sFlt-1 levels, changes in fatty acid gene expression and their master regulator *Ppara*, which also shows promoter methylation alterations in accordance with the gene expression. This is consistent with other models of developmental programming, for example, protein restriction.[17] These findings should warrant further investigations into the sFlt-1 contribution to the developmental programming of offspring health, namely via inspection of the second-generation offspring exposed to high sFlt-1 concentrations.

Conflict of Interest. The authors report no conflict of interest.

Ethical Standards. The authors assert that all procedures contributing to this work comply with the ethical standards of the relevant national guides on

the care and use of laboratory rats and has been approved by the Institutional Committee for Animal Ethical Experiments of the University of Groningen.

Supplementary materials. To view supplementary material for this article, please visit https://doi.org/10.1017/S2040174418000831

References

1. Godfrey KM, Gluckman PD, Hanson MA. Developmental origins of metabolic disease: life course and intergenerational perspectives. *Trends Endocrinol Metab*. 2010; 21, 199–205.

2. Mennitti LV, Oyama LM, Lopez de Oliveira J, *et al*. Oligofructose supplementation during pregnancy and lactation impairs offspring development and alters the intestinal properties of 21-d-old pups. *Lipids Health Dis*. 2014; 13, 26.

3. Florath I, Kohler M, Weck MN, *et al*. Association of pre- and post-natal parental smoking with offspring body mass index: an 8-year follow-up of a birth cohort. *Pediatr Obes*. 2014; 9, 121–134.

4. Byers BD, Betancourt A, Lu F, *et al*. The effect of prepregnancy obesity and sFlt-1-induced preeclampsia-like syndrome on fetal programming of adult vascular function in a mouse model. *Am J Obstet Gynecol*. 2009; 200, 432.e1–432.e7.

5. Werneck AO, Silva DRP, Collings PJ, *et al*. Birth weight, biological maturation and obesity in adolescents: a mediation analysis. *J Dev Orig Health Dis*. 2017; 8, 502–507.

6. Leddy MA, Power ML, Schulkin J. The impact of maternal obesity on maternal and fetal health. *Rev Obs Gynecol*. 2008; 1, 170–178.

7. Loaiza S, Coustasse A, Urrutia-Rojas X, Atalah E. Birth weight and obesity risk at first grade in a cohort of Chilean children. *Nutr Hosp*. 2011; 26, 214–219.

8. Reynolds LJ, Pollack RI, Charnigo RJ, *et al*. Increased birth weight is associated with altered gene expression in neonatal foreskin. *J Dev Orig Health Dis*. 2017; 8, 575–583.

9. Rajakumar A, Michael HM, Rajakumar PA, *et al*. Extra-placental expression of vascular endothelial growth factor receptor-1 (Flt-1) and soluble Flt-1 (sFlt-1), by peripheral blood mononuclear cells (PBMCs) in normotensive and preeclamptic pregnant women. *Placenta*. 2005; 26, 563–573.

10. Odegard RA, Vatten LJ, Nilsen ST, Salvesen KÅ, Austgulen R. Preeclampsia and fetal growth. *Obstet Gynecol*. 2000; 96, 950–955.

11. Hertig A, Berkane N, Lefevre G, *et al*. Maternal serum sFlt1 concentration is an early and reliable predictive marker of preeclampsia. *Clin Chem*. 2004; 50, 1702–1703.

12. Shibuya M. Vascular endothelial growth factor receptor-1 (VEGFR-1/Flt-1): a dual regulator for angiogenesis. *Angiogenesis*. 2006; 9, 225–230.

13. Bytautiene E, Bulayeva N, Bhat G, *et al*. Long-term alterations in maternal plasma proteome after sFlt1-induced preeclampsia in mice. *Am J Obstet Gynecol*. 2013; 208, 1–10.

14. Kuhnel E, Kleff V, Stojanovska V, *et al*. Placental-specific overexpression of sFlt-1 alters trophoblast differentiation and nutrient transporter expression in an IUGR mouse model. *J Cell Biochem*. 2017; 118, 1316–1329.

15. Maynard SE, Min J, Merchan J, *et al*. Excess placental soluble fms-like tyrosine kinase 1 (sFlt1) may contribute to endothelial dysfunction, hypertension, and proteinuria in preeclampsia. *J Clin Invest*. 2003; 111, 649–658.

16. Sartor MA, Tomlinson CR, Wesselkamper SC, *et al*. Intensity-based hierarchical Bayes method improves testing for differentially expressed genes in microarray experiments. *BMC Bioinformatics*. 2006; 7, 538.

17. Lillycrop KA, Phillips ES, Torrens C, *et al*. Feeding pregnant rats a protein-restricted diet persistently alters the methylation of specific cytosines in the hepatic PPAR alpha promoter of the offspring. *Br J Nutr*. 2008; 100, 278–282.

18. Lu F, Longo M, Tamayo E, *et al*. The effect of over-expression of sFlt-1 on blood pressure and the occurrence of other manifestations of preeclampsia in unrestrained conscious pregnant mice. *Am J Obstet Gynecol*. 2007; 196, 396.e1–396.e7.

19. Levine RJ, Maynard SE, Qian C, *et al*. Circulating angiogenic factors and the risk of preeclampsia. *N Engl J Med*. 2004; 350, 672–683.

20. Cohen E, Baerts W, Van Bel F. Brain-sparing in intrauterine growth restriction: considerations for the neonatologist. *Neonatology*. 2015; 108, 269–276.

21. Giussani DA. The fetal brain sparing response to hypoxia: physiological mechanisms. *J Physiol*. 2016; 594, 1215–1230.

22. Boito S, Struijk PC, Ursem NTC, Fedele L, Wladimiroff JW. Fetal brain/liver volume ratio and umbilical volume flow parameters relative to normal and abnormal human development. *Ultrasound Obstet Gynecol*. 2003; 21, 256–261.

23. Salam RA, Das JK, Bhutta ZA. Impact of intrauterine growth restriction on long-term health. *Curr Opin Clin Nutr Metab Care*. 2014; 17, 249–254.

24. Stojanovska V, Scherjon SA, Plösch T. Preeclampsia as modulator of offspring health. *Biol Reprod*. 2016; 94, 53–53.

25. Simmons RA, Templeton LJ, Gertz SJ. Intrauterine growth retardation leads to the development of type 2 diabetes in the rat. *Diabetes*. 2001; 50, 2279–2286.

26. Ozanne SE, Dorling MW, Wang CL, Petry CJ. Depot-specific effects of early growth retardation on adipocyte insulin action. *Horm Metab Res*. 2000; 32, 71–75.

27. Von Beckerath AK, Kollmann M, Rotky-Fast C, *et al*. Perinatal complications and long-term neurodevelopmental outcome of infants with intrauterine growth restriction. *Am J Obstet Gynecol*. 2013; 208, 130.e1–130.e6.

28. Rajakumar A, Powers RW, Hubel CA, *et al*. Novel soluble Flt-1 isoforms in plasma and cultured placental explants from normotensive pregnant and preeclamptic women. *Placenta*. 2009; 30, 25–34.

29. Wallner W, Sengenberger R, Strick R, *et al*. Angiogenic growth factors in maternal and fetal serum in pregnancies complicated with intrauterine growth restriction. *Clin Sci*. 2007; 112, 51–57.

30. Bergen NE, Bouwland-Both MI, Steegers-Theunissen RP, *et al*. Early pregnancy maternal and fetal angiogenic factors and fetal and childhood growth: the generation R study. *Hum Reprod*. 2015; 30, 1302–1313.

31. Boutsikou T, Malamitsi-Puchner A, Economou E, *et al*. Soluble vascular endothelial growth factor receptor-1 in intrauterine growth restricted fetuses and neonates. *Early Hum Dev*. 2006; 82, 235–239.

32. Renaud HJ, Cui JY, Lu H, Klaassen CD. Effect of diet on expression of genes involved in lipid metabolism, oxidative stress, and inflammation in mouse liver-insights into mechanisms of hepatic steatosis. *PLoS One*. 2014; 9, e88584.

33. Champier J, Claustrat F, Nazaret N, Montange MF, Claustrat B. Folate depletion changes gene expression of fatty acid metabolism, DNA synthesis, and circadian cycle in male mice. *Nutr Res*. 2012; 32, 124–132.

34. Grygiel-Górniak B. Peroxisome proliferator-activated receptors and their ligands: nutritional and clinical implications—a review. *Nutr J*. 2014; 13, 17.

35. Contreras AV, Torres N, Tovar AR. PPAR-α as a key nutritional and environmental sensor for metabolic adaptation. *Adv Nutr*. 2013; 4, 439–452.

36. Narravula S, Colgan SP. Hypoxia-inducible factor 1-mediated inhibition of peroxisome proliferator-activated receptor expression during hypoxia. *J Immunol*. 2001; 166, 7543–7548.

37. Lendvai Á, Deutsch MJ, Plösch T, Ensenauer R. The peroxisome proliferator-activated receptors under epigenetic control in placental metabolism and fetal development. *Am J Physiol Endocrinol Metab*. 2016; 310, E797–E810.

38. Magee TR, Han G, Cherian B, *et al*. Down-regulation of transcription factor peroxisome proliferator-activated receptor in programmed hepatic lipid dysregulation and inflammation in intrauterine growth-restricted offspring. *Am J Obstet Gynecol*. 2008; 199, 271e1–271e5.